arXiv:2105.13923v2 [physics.data-an] 14 Jan 2022

Nested sampling for frequentist computation: fast estimation of small *p*-values

Andrew Fowlie
*Department of Physics and Institute of Theoretical Physics, Nanjing Normal University, Nanjing, Jiangsu 210023, China**

Sebastian Hoof
Institut für Astrophysik, Georg-August-Universität Göttingen, Friedrich-Hund-Platz 1, 37077 Göttingen, Germany

Will Handley
Cavendish Laboratory & Kavli Institute for Cosmology, University of Cambridge, JJ Thomson Avenue, Cambridge, CB3 0HE, United Kingdom

We propose a novel method for computing p-values based on nested sampling (NS) applied to the sampling space rather than the parameter space of the problem, in contrast to its usage in Bayesian computation. The computational cost of NS scales as $\log^2 1/p$, which compares favorably to the $1/p$ scaling for Monte Carlo (MC) simulations. For significances greater than about 4σ in both a toy problem and a simplified resonance search, we show that NS requires orders of magnitude fewer simulations than ordinary MC estimates. This is particularly relevant for high-energy physics, which adopts a 5σ gold standard for discovery. We conclude with remarks on new connections between Bayesian and frequentist computation and possibilities for tuning NS implementations for still better performance in this setting.

I. INTRODUCTION

For decades, p-values have played a vital role in the discovery of new phenomena in high-energy physics (HEP) [1–6] as well as many other fields and disciplines. A p-value is the probability under a null hypothesis of observing results that are at least as "extreme" as the observed data. When the observed p-value is smaller than a pre-specified threshold α we reject the null hypothesis and claim a discovery.

As popularized by the Higgs boson discovery [7, 8], HEP usually requires $\alpha \sim 10^{-7}$, also known as the "5σ rule" [9].[1] Establishing a discovery thus requires the computation of $p \lesssim 10^{-7}$. This exposes difficulties in standard approaches to computing p-values, including the look-elsewhere effect [see e.g., 10], broken assumptions in popular asymptotic results [see e.g., 11] and the computational cost of computing p-values through Monte Carlo (MC) simulations. To overcome these problems, semi-analytic asymptotic formulae were developed alongside the Higgs searches [e.g., Gross–Vitells 12].

However, as discussed in the reviews [3–5], MC simulations are often unavoidable, as the asymptotic formulae make assumptions that often do not hold or that are difficult to check [13]. Straightforward examples include small sample sizes that cannot justify taking the asymptotic limit or when the hypotheses under consideration are not nested. For example, MC simulations were used by ATLAS and CMS at the LHC in e.g., searches for deviations from the Standard Model (SM) of particle physics [14, 15], searches for supersymmetry [16] and measurements of the Higgs boson's properties [16, 17]. Outside collider physics, they were used in searches for dark matter by the XENON collaboration [18, 19] and in astronomy by Fermi-LAT [20] and IceCube [21]. Lastly, MC simulations are used in global fits in particle physics e.g., [22–27], including GFITTER fits of the SM [28].

In this *Letter* we present a novel technique for computing global or local p-values based on nested sampling (NS) that in some regimes performs exponentially better than MC simulations. A basic implementation of our algorithm, including the examples provided in this *Letter*, is available on Github [29].

II. *P*-VALUES

Mathematically, p-values can be defined as the probability that a test-statistic (TS) λ is at least as great as the *observed* TS $\lambda^\star$ assuming that the null hypothesis H_0 is true,

$$p = P(\lambda \geq \lambda^\star \,|\, H_0)\,. \tag{1}$$

The task at hand is therefore to determine a tail probability from the sampling distribution of λ under H_0.

A. *P*-values from Monte Carlo simulations

Using MC simulations to determine the sampling distribution requires no asymptotic assumptions and provides

[1] In HEP, it is conventional to convert p-values into significances by the rule $Z = \Phi^{-1}(1-p)$, where Φ is the standard normal cumulative distribution function.

a robust and reliable p-value estimate [10]. These estimates obey binomial statistics since for each simulation either $\lambda \geq \lambda^\star$ or not. The p-value can then be estimated by $\hat{p} = m/n$ for m occurrences of $\lambda \geq \lambda^\star$ from n simulations. Evidently, a meaningful estimate requires at least $1/p$ simulations as the fractional error on $\hat{p}$ is of order of the Wald estimate,

$$\frac{\Delta p}{p} = \sqrt{\frac{1/p}{n}}\,. \tag{2}$$

See [30] for further discussion of errors for binomial parameters.

B. *P*-values from nested sampling

The nested sampling (NS) algorithm [31, 32] has primarily enjoyed success as a tool for computing the Bayesian evidence (see e.g. [33]), which is estimated through an identity involving the volume variable

$$X(\mathcal{L}^\star) = \int_{\mathcal{L}(\boldsymbol{\theta})>\mathcal{L}^\star} \pi(\boldsymbol{\theta})\,\mathrm{d}\boldsymbol{\theta}\,, \tag{3}$$

where π is the prior distribution, $\mathcal{L}$ is the likelihood and $\boldsymbol{\theta}$ are the model parameters. The threshold $\mathcal{L}^\star$ increases at each iteration of the algorithm. A scheme to estimate X lies at the heart of NS. See [34] for a recent review.

To understand why this is useful for p-value calculations, let us re-interpret Eq. (3) in a frequentist context. Rather than thinking of it as an integral over the parameter space, consider it as an integral over the sampling space. To give a concrete example, if we wish to simulate five Gaussian measurements, the sampling space would be five-dimensional and $\boldsymbol{\theta}$ would consist of the five simulated Gaussian measurements $\mathbf{x}$ rather than model parameters. We thus re-write Eq. (3) as

$$p = P(\lambda > \lambda^\star \,|\, H_0) = \int_{\lambda(\mathbf{x})>\lambda^\star} p(\mathbf{x}\,|\,H_0)\,\mathrm{d}\mathbf{x}\,, \tag{4}$$

which allows us to use NS to estimate p-values. A comparison of Eqs. (3) and (4) reveals that the pseudo-data $\mathbf{x}$ play the role of the model parameters $\boldsymbol{\theta}$, the sampling distribution of the pseudo-data $p(\mathbf{x}\,|\,H_0)$ plays the role of the prior and, lastly, the TS $\lambda(\mathbf{x})$ plays the role of the likelihood. Thus in the Bayesian setting, the volume variable in Eq. (3) is the fraction of the prior in which the likelihood exceeds a threshold, whereas in the frequentist one in Eq. (4), it is the fraction of the sampling distribution in which the TS exceeds a threshold.

The NS scheme for a statistical estimate of the volume variable works as follows. First, we draw $n_\mathrm{live} \sim \mathcal{O}(100\text{–}1000)$ "live points" from the sampling space. The parameter n_live acts as a resolution parameter, such that the runtime scales approximately as n_live, the uncertainty as $1/\sqrt{n_\mathrm{live}}$ and the chances of missing modes in multimodal problems as $1/n_\mathrm{live}$. At each subsequent iteration, the live point with the least extreme TS is replaced by one with a more extreme TS drawn from the sampling space (i.e. a draw from the constrained prior). This continues until iteration n_iter, when the least extreme TS among the live points exceeds the observed TS. We estimate the p-value using the usual NS estimate of the volume,[2]

$$p = X(\lambda^\star) \simeq \prod_{i=1}^{n_\mathrm{iter}} \mathrm{e}^{-1/n_\mathrm{live}} = \mathrm{e}^{-n_\mathrm{iter}/n_\mathrm{live}}\,. \tag{5}$$

Thus NS decomposes a tiny p-value into a product of n_iter moderate factors. This algorithm is shown schematically in Algorithm 1.

ALGORITHM 1. Schematic nested sampling algorithm for estimating p-values.

```
Draw n_live sets of pseudo-data from the sampling distribution — the live points;
Initialize n_iter = 0;
repeat
    n_iter = n_iter + 1;
    Find the minimum TS λ_min amongst the live points;
    Replace live point corresponding to λ_min by one drawn from the sampling distribution subject to λ > λ_min;
until λ_min ≥ λ*;
return Estimate of p = e^{-n_iter/n_live};
```

In the NS algorithm, n_iter is approximately Poisson-distributed with expectation value and variance both equal to $n_\mathrm{live} \log 1/p$. From Eq. (5) we see that $\log p$ follows a normal distribution with error

$$\frac{\Delta p}{p} \approx \Delta \log p = \frac{\Delta n_\mathrm{iter}}{n_\mathrm{live}} = \sqrt{\frac{\log 1/p}{n_\mathrm{live}}}\,, \tag{6}$$

with the approximation holding when $\Delta p/p \lesssim 1$. However, the number of TS evaluations required in an NS run n_eval must be proportional to the number of iterations before stopping. In fact, from the known properties of NS,

$$n_\mathrm{eval} = n_\mathrm{iter}/\epsilon = (n_\mathrm{live} \log 1/p)/\epsilon\,, \tag{7}$$

where ϵ denotes a problem-specific efficiency factor.[3] Thus we actually have

$$\frac{\Delta p}{p} \approx \Delta \log p = \sqrt{\frac{\log^2 1/p}{\epsilon\, n_\mathrm{eval}}}\,. \tag{8}$$

[2] This follows from $\mathrm{e}^{\langle \log X \rangle}$, i.e., from an unbiased estimator of $\log X$.

[3] This neglects the (generally negligible) n_live evaluations required for the initial live points.

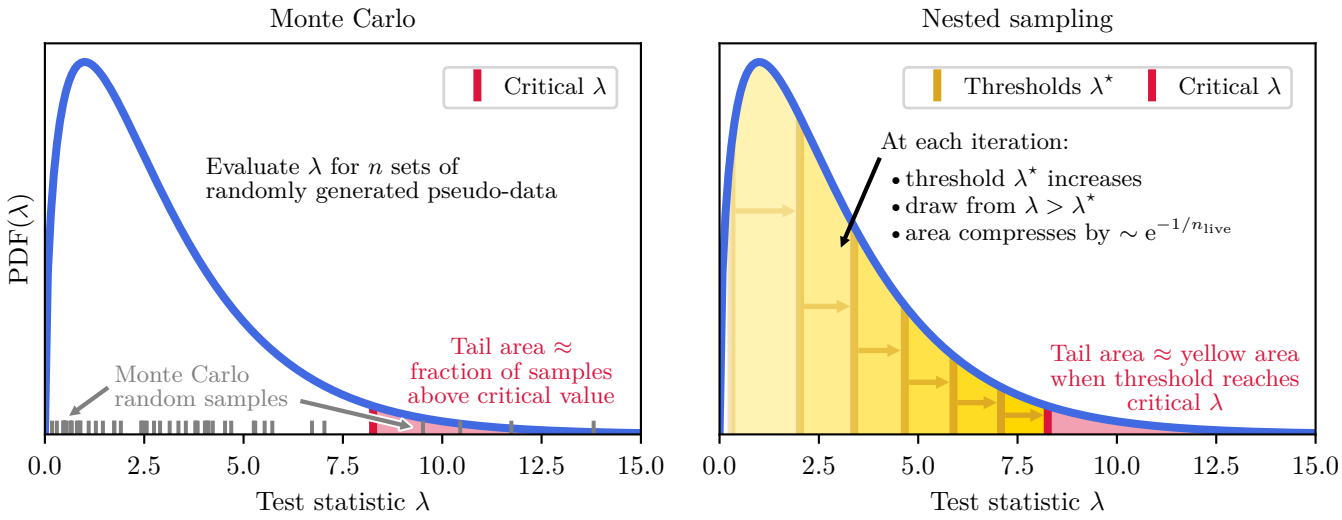


FIG. 1. Schematic illustration of MC (*left*) and NS (*right*) methods for computing p-values. The blue curve represents the probability distribution of the test statistic λ. The observed, critical value of λ is indicated by a thick, red, vertical line and the area beyond it (red shaded region) is the p-value. The shaded yellow region in the right panel illustrates the compression of the area under the curve at each step of the NS algorithm (progressively darker shading).

To compare the theoretical performances of MC and NS, we consider the ratio of the number of evaluations required to achieve a fixed relative error on the p-value. Note that the TS could be based on the profiled likelihood such that each evaluation could involve a complicated minimization over the actual model parameters. Comparing the error estimates from Eqs. (2) and (6), we find a ratio of

$$\frac{\text{Evaluations for NS}}{\text{Evaluations for MC}} = \frac{(\log^2 1/p)/\epsilon}{1/p} \,. \tag{9}$$

For small enough p-values, NS has the potential to beat MC by an arbitrarily large margin. The efficiency factor, however, could spoil NS performance in realistic applications and depends the details of the NS implementation and the problem at hand, including the dimensionality. Because of these complications, we will consider the computational performance for two benchmark cases in Section III.

We summarize and illustrate the idea of "nested p-value computation" in comparison to MC in Fig. 1. We want to emphasize that, in the context of this work, *NS is merely a mathematical tool.*

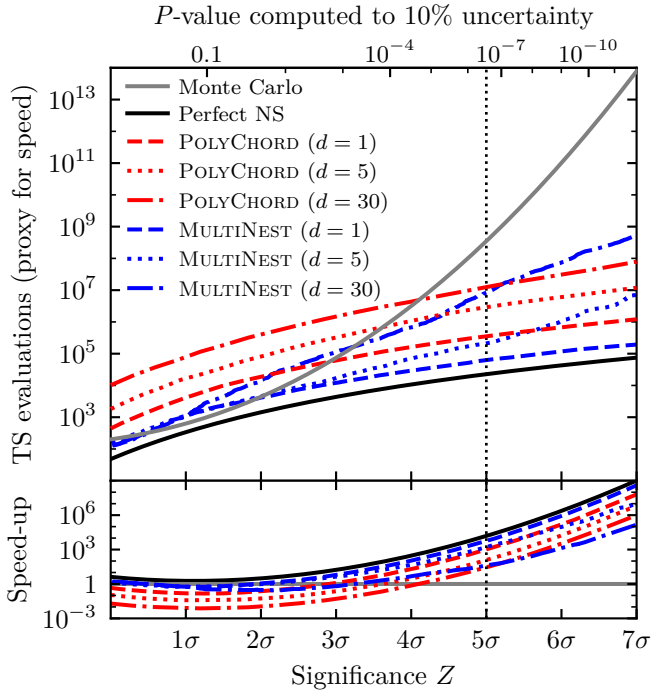


FIG. 2. Performance of NS versus MC for the χ^2_d example. The performance of perfect NS and MC are independent of d. Performance was measured by the TS evaluations required to compute the p-value to within 10% uncertainty.

III. APPLICATIONS AND PERFORMANCE

To illustrate how to use our algorithm and to assess its performance, we conduct two case studies. First, we consider the example of multi-dimensional Gaussians. Second we apply our algorithm to a simplified version of a resonance search.

A. Gaussian measurements

Consider the p-value associated with d independent Gaussian measurements. We define the TS as the sum of the d associated chi-squared variates. Thus $\lambda \sim \chi^2_d$ and

the p-value may be computed analytically. We construct the problem in NS by mapping from draws from a d dimensional unit hypercube with coordinates $x_i \sim \mathcal{U}(0,1)$, to d draws from a chi-squared distribution via $z_i = F^{-1}_{\chi^2_1}(x_i)$ for $i = 1, \ldots, d$ such that $z_i \sim \chi^2_1$ and $\lambda = \sum z_i \sim \chi^2_d$.

We show the performance of NS and MC on this problem in Fig. 2 as a function of the significance. The performance of perfect NS (in which we suppose that one could sample directly from the constrained prior) and MC are independent of d. The performance of real implementations of NS however depends on d, as they must utilize numerical schemes for sampling from the d-dimensional constrained prior. We demonstrate the performance of MultiNest [35, 36] and PolyChord [37], which utilize ellipsoidal and slice sampling, respectively.[4] We use the number of TS evaluations as a measure of performance, which is sensible when the computational cost is dominated by TS evaluations. While this is usually a good assumption in practice, we note that MultiNest appears to suffer from a greater computational overhead than PolyChord in our example, possibly due to the linear algebra operations required for clustering live points and constructing ellipsoids, especially for $d = 30$ over 5σ. For this case, MultiNest was about 2,000 times slower than PolyChord (with sizeable variability in run times), which significantly exceeds the ratio of TS evaluations needed.

B. Resonance search

The original Higgs discovery by the ATLAS Collaboration [7] is a typical example of a resonance search (testing a spectrum for the presence of a signal above a smooth background), which includes the common complications of parameters on the boundary of the parameter space and the look-elsewhere effect. Here, the null hypothesis H_0 corresponds to the Standard Model (SM) hypothesis, with a known shape and an unknown nuisance parameter b, the total number of background events. The alternative hypothesis H_1 is that of the SM background plus a Higgs boson with a Gaussian signal, with a known width but an unknown mass m_h and an unknown positive signal strength $s \geq 0$.[5] The null hypothesis lies at the $s = 0$ boundary. The data $\mathbf{x} = \{n_i\}$ consists of the Poisson-distributed observed counts n_i in the 30 bins shown in Figure 4 of [7]. The TS is the log-likelihood ratio

$$\lambda(\mathbf{x}) = 2 \log \left(\frac{\max P(\mathbf{x} \,|\, b, s, m_h)}{\max P(\mathbf{x} \,|\, b, s = 0)} \right) , \qquad (10)$$

where we maximize over all parameters for a given (pseudo-)data set $\mathbf{x}$.

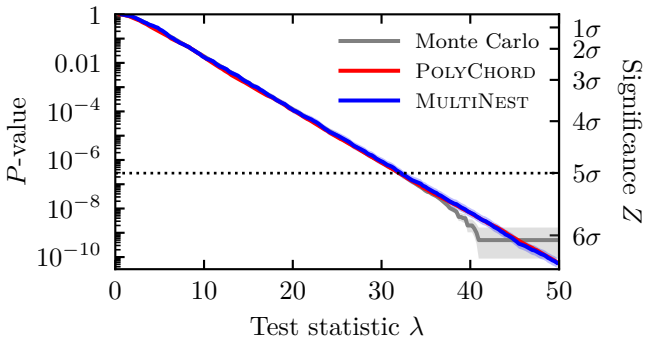


FIG. 3. Calibration of the resonance search TS. We show the estimated p-value with shaded uncertainties for MC simulations (gray; 2×10^9 samples), PolyChord (red; weighted average of four runs), and MultiNest (blue; single run).

In summary, the data space $\mathbf{x}$, and hence the pseudo-data sampling space, is 30-dimensional while the null and alternative models have only one and three model parameters respectively.

To compute p-values in the presence of a nuisance parameter [38], we plug in the best-fit value of the unknown nuisance parameter b in Eq. (1). We perform brute-force MC simulations and NS with MultiNest and PolyChord to calibrate the TS λ. The results are shown in Fig. 3.

To reach a TS of $\lambda = 50$ (6.5σ) PolyChord requires about 3×10^6 TS evaluations. MultiNest typically requires around 3.5×10^7 TS evaluations, i.e. an order of magnitude more. To achieve a similar level of uncertainty as a single NS run for $\lambda = 50$, where $\Delta \log_{10} p \approx 0.2$ for both MultiNest and PolyChord, we would require about 10^{11} MC simulations. Since this would be computationally fairly expensive, we only simulated 2×10^9 samples for Fig. 3.

The improved performance for NS vs MC in terms of TS evaluations is in line with Fig. 2 and also with CPU run times required: a typical PolyChord run took about 300 CPUh (equivalent hours on a single computing core) while the required 10^{11} MC simulations would take around 9.2×10^6 CPUh, such that we achieved a speed-up of about 31,000.

Note that the gradient of the linear slope in Fig. 2 also agrees with the asymptotic Gross–Vitells method [12], $\log p \approx c_0 - \frac{1}{2}\lambda$. Whilst this method may be used to efficiently compute p-values in the resonance search example, it is not applicable in other cases of interest [13]. As a concrete example, consider the goodness-of-fit test

[4] We changed the codes to stop once the required TS threshold was reached. While we chose n_{live} to achieve the desired uncertainty, we generally suggest to choose $n_{\text{live}} \geq \max(100, d)$. We set `efr` $= 0.3$ and `num_repeats` $= 5d$ and `do_clustering = False`. See the associated codes for our complete settings [29].

[5] In the original analysis, the signal is described by a Crystal Ball function and the background model is more complex [7].

of the SM plus Higgs hypothesis, which can be performed using the TS [39]

$$\lambda(\mathbf{x}) = -2\log\left(\frac{\max P(\mathbf{x}\,|\,b,s,m_h)}{P(\mathbf{x}\,|\,\mu_i = n_i)}\right), \qquad (11)$$

with b, s, and m_h are as in Eq. (10). We set the μ_i parameters in the Poisson distribution for each bin equal to the pseudo-counts data n_i in that bin. Since the μ_i are different from the model parameters of the Higgs hypothesis, these two models are not nested.

The naïve expectation for the goodness-of-fit test is that it follows a χ^2_d distribution with $d = 30 - 3 = 27$ degrees of freedom The implied critical value of the TS for 5σ ($p \approx 28.7 \times 10^{-8}$) is then $\lambda^\star \approx 80.8$. However, with direct MC simulations and PolyChord, we estimate the corresponding p-values to be $p = (8.4 \pm 1.0) \times 10^{-8}$ and $p = (6.6 \pm 1.1) \times 10^{-8}$, respectively, or around 5.3σ. This discrepancy from the asymptotic result should be anticipated, as the SM plus Higgs is not a linear model [40]. The six PolyChord runs that we used for this estimate took on average about 1.3×10^6 function calls and 220 CPUh. The CPU time per TS function call is consistent with our MC analysis, where we simulated 8.2×10^8 samples in total. The achieved speed-up of about 100 is consistent with Fig. 2.

IV. DISCUSSION AND CONCLUSIONS

In this *Letter*, we propose the use of nested sampling (NS) for computing p-values. Our proposal is compatible with readily available, established implementations of the NS algorithm. The most notable advantage of using NS is the order-of-magnitudes speed-up that can be achieved for small p-values of scientific importance in comparison with Monte Carlo (MC) simulations. This advantage can be traced to the fact that, despite their conceptual differences, p-values and the Bayesian evidence have one thing in common that makes them difficult to compute: *compression*. For the Bayesian evidence, the compression occurs between prior and posterior distributions, and is typically enormous if the data favor a narrow region of the parameter space. For p-values, the compression is from the whole sampling space to the region where the test statistic (TS) is greater than its observed value. By definition, the compression is enormous for small p-values.

We can understand the applicability of NS to compression problems in both Bayesian and frequentist settings as follows: simulating from the entire sampling distribution (or the entire prior in the Bayesian setting) is inefficient when the interesting region of sampling space is tiny. Conversely, simulating only from the region of interest (or from the posterior in the Bayesian setting) does not allow reliable inference about its relative size.

Heuristically, it is not surprising that successful strategies simulate from a series of distributions that form a path between e.g. the prior and posterior (see [41, 42] for further discussion). Since the constrained prior can be related to the p-value by Eq. (4), the sequence of constrained priors in NS naturally forms a path between the entire sampling space and the tiny tail area of interest corresponding to the p-value, which makes it particularly well-suited for frequentist computation. Path sampling in this manner is a generalization of importance sampling [42]. See [43] for related work on computing p-values through importance sampling and [36] for an importance sampling algorithm that uses NS draws.

We see three potential drawbacks when using NS in this setting. First, the data space in a realistic problem can be very high-dimensional. For example, a search for new particles at the LHC could look for evidence in a histogram containing 100 bins or more. While some implementations of the NS scheme potentially suffer from poor efficiency in higher dimensions, using e.g. NS with slice sampling achieves $\epsilon \propto 1/d$ behavior and has been applied successfully to problems with hundreds of dimensions [44].

Second, while an NS run with n_{live} live points can be efficiently parallelized into in principle as many as n_{live} runs with a single live point, those individual runs must proceed linearly.[6] By using exponentially large amounts of computational resources, it is therefore possible to make brute-force MC compute p-values faster than any realistic NS algorithm, albeit at significantly greater overall computational expense.

Lastly, there is a subtlety concerning substantial plateaus in the TS, that is, regions of sampling space that lead to an identical TS. In some NS implementations plateaus lead to faulty estimates of the volume variable [45], and thus would lead to faulty estimates of the p-value. In such cases, an implementation of NS that supports plateaus must be used or the p-value must be corrected using e.g., anesthetic [46].

Despite its drawbacks, the in-principle exponential improvement makes our method a valuable tool—in particular when considering small p-values. We demonstrated in practice that our algorithm can significantly reduce the computational burden of p-value calculations with the popular MultiNest and PolyChord algorithms. This allows for a straightforward adoption of our algorithm, encouraging more rigorous p-value calculations and potentially opening up problems that were previously computationally unfeasible.

[6] The uncertainty of the estimate, however, may be reduced by running the algorithm multiple times .

ACKNOWLEDGMENTS

AF was supported by an NSFC Research Fund for International Young Scientists grant 11950410509. SH was funded by the Alexander von Humboldt Foundation and the German Federal Ministry of Education and Research. WH was supported by a Royal Society University Research Fellowship. We used the Scientific Computing Cluster at GWDG, the joint data centre of Max Planck Society for the Advancement of Science (MPG) and the University of Göttingen. This work was also performed using the Cambridge Service for Data Driven Discovery (CSD3), part of which is operated by the University of Cambridge Research Computing on behalf of the STFC DiRAC HPC Facility (www.dirac.ac.uk). The DiRAC component of CSD3 was funded by BEIS capital funding via STFC capital grants ST/P002307/1 and ST/R002452/1 and STFC operations grant ST/R00689X/1. DiRAC is part of the National e-Infrastructure

* andrew.j.fowlie@njnu.edu.cn

[1] L. Lyons, *Statistics for Nuclear and Particle Physicists* (Cambridge University Press, 1986).

[2] G. Cowan, in *69th Scottish Universities Summer School in Physics: LHC Physics* (2013) pp. 321–355, arXiv:1307.2487 [hep-ex].

[3] K. Cranmer, in *2011 European School of High-Energy Physics* (2014) pp. 267–308, arXiv:1503.07622 [physics.data-an].

[4] R. D. Cousins, arXiv e-prints (2018), arXiv:1807.05996 [physics.data-an].

[5] P. Zyla *et al.* (Particle Data Group), PTEP **2020**, 083C01 (2020), "Chap. 40. Statistics by Glen Cowan".

[6] T. R. Junk and L. Lyons, Harvard Data Science Review **2**, 4 (2020), arXiv:2009.06864 [physics.data-an].

[7] G. Aad *et al.* (ATLAS), Phys. Lett. B **716**, 1 (2012), arXiv:1207.7214 [hep-ex].

[8] S. Chatrchyan *et al.* (CMS), Phys. Lett. B **716**, 30 (2012), arXiv:1207.7235 [hep-ex].

[9] L. Lyons, arXiv e-prints (2013), arXiv:1310.1284 [physics.data-an].

[10] S. Algeri, J. Conrad, D. A. van Dyk, and B. Anderson, JINST **11** (12), P12010, arXiv:1602.03765 [physics.data-an].

[11] G. Cowan, K. Cranmer, E. Gross, and O. Vitells, Eur. Phys. J. C **71**, 1554 (2011), [Erratum: Eur. Phys. J. C **73**, 2501 (2013)], arXiv:1007.1727 [physics.data-an].

[12] E. Gross and O. Vitells, Eur. Phys. J. C **70**, 525 (2010), arXiv:1005.1891 [physics.data-an].

[13] S. Algeri, J. Aalbers, K. D. Morâ, and J. Conrad, Nature Reviews Physics **2**, 245 (2020), arXiv:1911.10237 [physics.data-an].

[14] M. Aaboud *et al.* (ATLAS), Eur. Phys. J. **C79**, 120 (2019), arXiv:1807.07447 [hep-ex].

[15] A. M. Sirunyan *et al.* (CMS), Eur. Phys. J. C **81**, 629 (2021), arXiv:2010.02984 [hep-ex].

[16] S. Chatrchyan *et al.* (CMS), Phys. Rev. D **90**, 112001 (2014), arXiv:1405.3961 [hep-ex].

[17] S. Chatrchyan *et al.*, Phys. Rev. Lett. **110**, 081803 (2013), arXiv:1212.6639 [hep-ex].

[18] E. Aprile *et al.*, Phys. Rev. D **102**, 072004 (2020), arXiv:2006.09721 [hep-ex].

[19] D. Baxter *et al.*, arXiv e-prints (2021), arXiv:2105.00599 [hep-ex].

[20] A. Albert *et al.* (Fermi-LAT and DES Collaborations), Astrophys. J. **834**, 110 (2017), arXiv:1611.03184 [astro-ph.HE].

[21] A. Sharma and E. O'Sullivan (IceCube), PoS **ICRC2021**, 971 (2021), arXiv:2107.08159 [astro-ph.HE].

[22] P. Bechtle, J. E. Camargo-Molina, K. Desch, H. K. Dreiner, M. Hamer, M. Krämer, B. O'Leary, W. Porod, B. Sarrazin, T. Stefaniak, M. Uhlenbrock, and P. Wienemann, Eur. Phys. J. **C76**, 96 (2016), arXiv:1508.05951 [hep-ph].

[23] P. Athron, C. Balázs, A. Beniwal, J. E. Camargo-Molina, A. Fowlie, T. E. Gonzalo, S. Hoof, F. Kahlhoefer, D. J. E. Marsh, M. T. Prim, A. Scaffidi, P. Scott, W. Su, M. White, L. Wu, and Y. Zhang, JHEP **2021** (5), 159, arXiv:2007.05517 [astro-ph.CO].

[24] G. Isidori, D. Lancierini, P. Owen, and N. Serra, Phys. Lett. B **822**, 136644 (2021), arXiv:2104.05631 [hep-ph].

[25] M. Blennow, P. Coloma, P. Huber, and T. Schwetz, JHEP **2014**, 28, arXiv:1311.1822 [hep-ph].

[26] J. Elevant and T. Schwetz, JHEP **09**, 016, arXiv:1506.07685 [hep-ph].

[27] P. Coloma, P. Huber, and T. Schwetz, Eur. Phys. J. **C81**, 2 (2021), arXiv:2008.06083 [hep-ph].

[28] M. Baak, J. Cúth, J. Haller, A. Hoecker, R. Kogler, K. Mönig, M. Schott, and J. Stelzer, Eur. Phys. J. **C74**, 3046 (2014), arXiv:1407.3792 [hep-ph].

[29] A. Fowlie, S. Hoof, and W. Handley, Code and data for "nested sampling for frequentist computation", `https://github.com/andrewfowlie/ns_for_p_values` (2021).

[30] L. D. Brown, T. T. Cai, and A. DasGupta, Statistical Science **16**, 101 (2001).

[31] J. Skilling, in *American Institute of Physics Conference Series*, American Institute of Physics Conference Series, Vol. 735, edited by R. Fischer, R. Preuss, and U. V. Toussaint (2004) pp. 395–405.

[32] J. Skilling, Bayesian Analysis **1**, 833 (2006).

[33] R. E. Kass and A. E. Raftery, J. Am. Statist. Assoc. **90**, 773 (1995).

[34] J. Buchner, arXiv e-prints (2021), arXiv:2101.09675 [stat.CO].

[35] F. Feroz and M. P. Hobson, Mon. Not. Roy. Astron. Soc. **384**, 449 (2008), arXiv:0704.3704 [astro-ph].

[36] F. Feroz, M. P. Hobson, E. Cameron, and A. N. Pettitt, The Open Journal of Astrophysics (2013), arXiv:1306.2144 [astro-ph.IM].

[37] W. J. Handley, M. P. Hobson, and A. N. Lasenby, Mon. Not. Roy. Astron. Soc. **450**, L61 (2015), arXiv:1502.01856 [astro-ph.CO].

[38] L. Demortier, in *PHYSTAT-LHC Workshop on Statistical Issues for LHC Physics* (2008) pp. 23–33.

[39] S. Baker and R. D. Cousins, Nucl. Instrum. Meth. **221**, 437 (1984).

[40] R. Andrae, T. Schulze-Hartung, and P. Melchior, arXiv e-prints (2010), arXiv:1012.3754 [astro-ph.IM].

[41] E. Cameron and A. N. Pettitt, Statistical Science **29**, 397 (2014), arXiv:1301.6450 [stat.ME].

[42] A. Gelman and X.-L. Meng, Statistical Science **13**, 163 (1998).
[43] M. Wiebusch, Computer Physics Communications **184**, 2438 (2013), arXiv:1207.1446 [hep-ph].
[44] K. Javid, W. Handley, M. Hobson, and A. Lasenby, arXiv e-prints (2020), arXiv:2004.12211 [stat.ML].
[45] A. Fowlie, W. Handley, and L. Su, Mon. Not. Roy. Astron. Soc. **503**, 1199 (2021), arXiv:2010.13884 [stat.CO].
[46] W. Handley, J. Open Source Softw. **4**, 1414 (2019), arXiv:1905.04768 [astro-ph.IM].